Title

Discovery and Characterization of Antibody Probes of Module 2 of the 6–Deoxyerythronolide B Synthase

Journal

Biochemistry, 62(11)

ISSN

0006-2960

Authors

Guzman, Katarina M
Cogan, Dillon P
Brodsky, Krystal L
et al.

Publication Date

2023-06-06

DOI

10.1021/acs.biochem.3c00156

Peer reviewed

HHS Public Access

Author manuscript

Biochemistry. Author manuscript; available in PMC 2024 June 06.

Published in final edited form as:

Biochemistry. 2023 June 06; 62(11): 1589–1593. doi:10.1021/acs.biochem.3c00156.

Discovery and Characterization of Antibody Probes of Module 2 of the 6-Deoxyerythronolide B Synthase

Katarina M. Guzman[a], **Dillon P. Cogan**[b], **Krystal L. Brodsky**[b], **Alexander M. Soohoo**[a], **Xiuyuan Li**[b,#], **Natalia Sevillano**[c], **Irimpan I. Mathews**[d], **Khanh P. Nguyen**[b], **Charles S. Craik**[c], **Chaitan Khosla**[a,b,e,*]

[a]Department of Chemical Engineering, Stanford University, Stanford, California 94305, United States

[b]Department of Chemistry, Stanford University, Stanford, California 94305, United States

[c]Department of Pharmaceutical Chemistry, University of California San Francisco, San Francisco, California 94158, United States

[d]Stanford Synchrotron Radiation Lightsource, SLAC National Accelerator Laboratory, Stanford University, Menlo Park, California 94025, United States

[e]Sarafan ChEM-H, Stanford University, Stanford, California 94305, United States

Abstract

Fragment antigen-binding domains of antibodies (F_{ab}s) are powerful probes of structure-function relationships of assembly-line polyketide synthases (PKSs). We report the discovery and characterization of F_{ab}s interrogating the structure and function of the ketosynthase-acyltransferase (KS-AT) core of Module 2 of the 6-deoxyerythronolide B synthase (DEBS). Two F_{ab}s (AC2 and BB1) were identified to potently inhibit the catalytic activity of Module 2. Both AC2 & BB1 were found to modulate ACP-mediated reactions catalyzed by this module, albeit by distinct mechanisms. AC2 primarily affects the rate (k_{cat}), whereas BB1 increases the K_M of an ACP-mediated reaction. A third F_{ab}, AA5, binds to the KS-AT fragment of DEBS Module 2 without altering either parameter; it is phenotypically reminiscent of a previously characterized F_{ab}, 1B2, shown to principally recognize the N-terminal helical docking domain of DEBS Module 3. Crystal structures of AA5 and 1B2 bound to the KS-AT fragment of Module 2 were solved to 2.70 and 2.65 Å resolution, respectively, and revealed entirely distinct recognition features of

[*]**Corresponding Author** khosla@stanford.edu.

[#]**Present Addresses** X.L.: Department of Chemistry and Chemical Biology, Harvard University, Cambridge, Massachusetts 02138, United States

Author Contributions

The manuscript was primarily written through contributions of Katarina Guzman and Chaitan Khosla. Remaining authors provided experimental assistance and/or guidance. All authors have given approval to the final version of the manuscript.

The authors declare no competing financial interest.

ASSOCIATED CONTENT

Supporting Information. Plasmid and protein sequences; enzymatic assay, protein purification, crystallography methods; NDK-SNAC synthesis; Supplementary Figures. This material is available free of charge via the Internet at http://pubs.acs.org.

Accession Codes. 6-deoxyerythronolide-B synthase EryA1, modules 1 and 2 (Uniprot, Q03131 · ERYA1_SACER); 6-deoxyerythronolide-B synthase EryA3, modules 5 and 6 (Uniprot, Q03133 · ERYA3_SACER); 1B2 Antibody (PDB 6C9U); 1B2-D(3)KS_2-AT_2 (PDB ID 8EE0); AA5-D(3)KS_2-AT_2 (PDB ID 8EE1); ACP2 (PDB 2JU2).

the two antibodies. The new tools and insights reported here pave the way towards advancing our understanding of the structure-function relationships of DEBS Module 2, arguably the most well-studied module of an assembly-line PKS.

Graphical Abstract

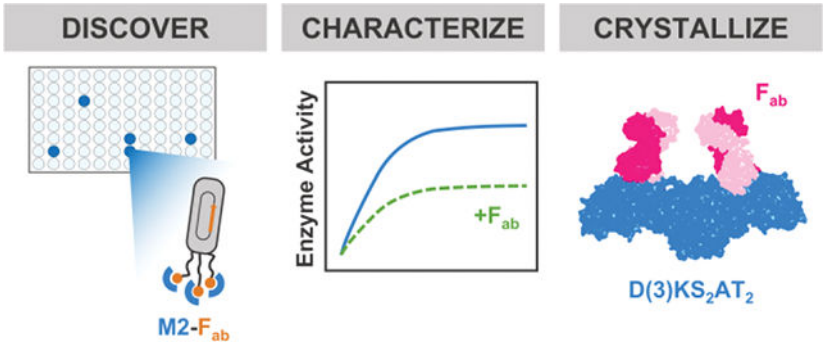

Keywords

Crystallography; Fragment-Antigen Binding Domains; Polyketide Synthase

Assembly-line polyketide synthases (PKSs) are multi-enzyme systems that synthesize structurally complex polyketide natural products, many of which have found therapeutic utility (1). Engineering assembly-line PKSs to produce novel bioactive agents has therefore been a longstanding goal, albeit a challenging one due to their sheer complexity and our limited understanding of their structure-function relationships. To advance this frontier, our laboratory and others have focused on achieving a fundamental understanding of the core mechanisms underlying the enzymology of assembly-line PKSs. Specifically, each PKS module of an assembly line harbors a ketosynthase (KS), an acyltransferase (AT), and an acyl carrier protein (ACP) domain that collaborate to elongate the growing polyketide chain via a decarboxylative C-C bond forming reaction with an unsubstituted or substituted malonyl extender unit (2). Additional enzymatic domains (e.g., ketoreductase (KR), dehydratase (DH), enoyl reductase (ER)) may also be present in some but not all modules of assembly-line PKSs (3–5). Owing to the universality of the chain elongation process, we have sought to understand the mechanisms by which the KS, AT, ACP, and their covalently bound acyl-chain species interact with each other in the context of the catalytic cycle of a PKS module (Figure S1).

Over the past two decades, X-ray crystallography and single-particle cryo-electron microscopy (cryoEM) have been especially powerful structural tools for structure-function analysis of assembly-line PKSs (6–17). More recent structural efforts have also relied on the use of fragment antigen-binding domains of antibodies (F_{ab}s) as chaperones for crystallography and cryoEM (6, 12–15). For example, the F_{ab} 1B2 binds to the N-terminal helical docking domain of Module 3 of the 6-deoxyerythronolide B synthase (DEBS; Figure 1) and has proven invaluable for visualizing entire modules of two unrelated PKSs, the lasalocid PKS (13) and DEBS (14). We therefore sought to discover additional antibody

probes to enhance our understanding of the KS-AT core of a representative assembly-line PKS module.

Analogous to our previous phage display library screen of F_{ab}s (3.7×10^{10}) against DEBS modules 1 and 3 (6, 12, 15), three unique F_{ab}s (AA5, AC2, and BB1) against DEBS Module 2 were identified (Figure 1). To stabilize Module 2 in its homodimeric state in the absence of the remainder of the DEBS 1 protein (Figure S1), this stand-alone module was fused to the N-terminal coiled-coil docking domain from Module 3 (hereafter referred to as D(3)-Module 2).

Binding analysis using size exclusion chromatography (SEC) revealed that all three F_{ab}s recognized the homodimeric D(3)KS_2-AT_2 fragment of D(3)-Module 2 (representative data for AA5 is shown in Figure 2; data for other antibodies is shown in Figure S2). Antibody recognition was quantified via ELISA with apparent K_D values of AA5, AC2, and BB1 being 5.7 ± 0.06, 1.6 ± 0.02, and 8.2 ± 0.07 nM, respectively (Figure S3).

The ability of all three F_{ab}s to bind homodimeric D(3)KS_2-AT_2 tightly highlights the power of phage display libraries of naïve F_{ab}s to yield high-affinity reagents. Control studies with a previously characterized F_{ab}, 1B2, which recognizes the D(3) docking domain of Module 3, validated our analysis of the newly isolated antibodies (Figure S4) (15).

To establish that AA5, AC2, and BB1 specifically recognized the KS-AT fragment of Module 2 and not its flanking D(3) domain, each antibody was counter-screened against D(5)KS_2-AT_2, a homodimeric construct harboring the distantly related N-terminal docking domain of Module 5 in lieu of D(3) (Figure S5). All three F_{ab}s described in this report (AA5, AC2, and BB1) retained their affinity for the latter protein, while 1B2 was unable to bind D(5)KS_2-AT_2 (Figure S6). From this data we concluded that AA5, AC2, and BB1 were specific for the KS-AT core of Module 2.

To investigate whether AA5, AC2, and BB1 inhibited the catalytic activity of Module 2, turnover of a truncated derivative of DEBS harboring its loading didomain, Module 1, and Module 2 fused to the terminal thioesterase (TE) domain was measured spectroscopically in the presence of each F_{ab} (15). As shown in Figure 3A, AC2 and BB1 but not AA5 inhibited turnover of this bimodular PKS.

As illustrated by the control 1B2 antibody, this assay is incapable of discriminating between inhibition of intermodular chain translocation between the ACP domain of Module 1 and the KS domain of Module 2 from inhibition of a core reaction (transacylation or elongation) catalyzed by KS_2-AT_2. To do so, the turnover of stand-alone Module 2-TE was assayed in the presence of a diffusible analog of its natural diketide substrate (hereafter referred to as NDK-SNAC, whose preparation is described in Figures S7–S13) (15, 18–20). AC2 and BB1 (but not AA5) inhibited Module 2-TE enzyme activity (Figure 3B). To further dissect this inhibition mechanism, Module 2 was dissociated into three fragments: D(3)KS_2-AT_2, KR_2, and ACP_2 (Figure S14). Prior efforts in our laboratory to reconstitute the catalytic activity of a PKS module from its dissected domains relied on ^{14}C radiolabeling or LC-MS assays (21). Here we were able to quantify the activity of Module 2 by monitoring NADPH consumption in the presence of a stoichiometric excess of ACP_2 (Figure S15). Under conditions where

neither KS acylation with its diketide substrate nor ACP acylation with a methylmalonyl extender unit nor β-ketoreduction of the elongated triketide product were rate-limiting, AC2 and BB1 inhibited turnover of dissociated Module 2 while AA5 did not (Figure 3C, Figure S16) (19, 22). Notably, the inhibitory mechanisms of AC2 and BB1 were different; whereas AC2 appeared to be a non-competitive inhibitor, the inhibitory effect of BB1 appeared predominantly competitive. The competitive nature of BB1 inhibition in this assay is distinct from its non-competitive inhibitory effect in the stand-alone M2-TE assay (Figure 3B). Taken together, our data suggests that TE-promoted substrate off-loading, not KS-promoted chain elongation, is rate limiting in the M2-TE turnover assay under saturating NDK-SNAC concentrations. This finding yet again highlights the utility of F_{ab}s as mechanistic probes for PKSs. Further analysis of the distinct inhibitory mechanisms of AC2 and BB1 is warranted.

While crystal growth from complexes comprised of KS_2-AT_2 and either AC2 or BB1 has proven elusive thus far, we took advantage of AA5 and 1B2 as crystallography chaperones to obtain co-crystals that diffracted to 2.70 and 2.65 Å, respectively (Figure 4, Table S1, Figure S17). In both cases the homodimeric KS_2-AT_2 protein crystallized in an extended architecture analogous to all previously characterized high-resolution structures of this didomain core of assembly-line PKS modules (13–15, 23).

Similar to its previously reported co-crystal structure with D(3)KS_3-AT_3, 1B2 predominantly made contact with the N-terminal docking domain of D(3)KS_2-AT_2 (Figure S18) (15). While D(3) was well-resolved in this co-crystal structure, it was not resolved in the AA5 co-crystal structure. Meanwhile, AA5 principally contacted the hydrolase subdomain of the AT in an orientation that was directed away from its active site Ser residue. Additional contacts were also observed with the KS-AT linker. The remarkably high affinity of AA5 for KS_2-AT_2 appears to be dominated by several polar contacts (Figure S19). Overall, this structure validates the non-inhibitory nature of AA5 binding to Module 2. No major conformational changes were observed between the two snapshots of the KS_2-AT_2 fragment (Figure S20, RMSD 1.44 Å). Slight variation between the two KS_2-AT_2 models can be attributed to AT flexibility; this type of rotation of the AT domain has been previously described (23–24). Modeling studies were undertaken with the previously reported NMR structure of ACP_2 (PDB ID 2JU2) (25) to gain insight into the specificity-determining residues at the KS/ACP interface of DEBS Module 2. Recently the cryoEM structure of DEBS Module 1 with the ACP stalled in the elongation state (PDB ID 7M7F), was reported (14). To simulate the analogous binding pose for DEBS Module 2, the KS_2-AT_2 didomain from PDB 8EE0 (in complex with F_{ab} 1B2) was superposed onto the KS_1-AT_1 didomain and the solution NMR structure of ACP_2 was superposed onto ACP_1 (Figure S21). In agreement with prior experimental data, the model revealed favorable interactions between Loop 1 of ACP_2 and the KS_2-AT_2 (26), further supporting our reported structures.

This is the first reported structure of the KS-AT didomain of DEBS Module 2, arguably the most extensively studied module of an assembly-line PKS to date (11, 25–28). Our results highlight the utility of F_{ab}s in studying PKSs. Three unique F_{ab}s (AA5, AC2, and BB1) that recognize the KS-AT fragment of DEBS Module 2 were characterized. AA5 was highlighted as a crystallography chaperone, meanwhile AC2 and BB1 have unique inhibitory properties that are useful mechanistic probes of Module 2. This module is known

to have an exceptionally broad substrate scope (27); further investigations into this property are warranted in a manner that is enabled by our reported structures and crystallographic chaperones.

Supplementary Material

Refer to Web version on PubMed Central for supplementary material.

ACKNOWLEDGMENT

We thank members of the Khosla Lab for thoughtful discussions. This work was supported by the National Institutes of Health (NIH) grant GM141799 (to C.K.), and GM136039 (to D.P.C.), a Stanford Graduate Fellowship (SGF) Award (to K.M.G.), and National Science Foundation Graduate Research Fellowship under Grant DGE-1656518 (to A.M.S.). This work utilized the Stanford Cancer Institute Proteomics/Mass Spectrometry Shared Resource, which is supported by NIH Grant P30 CA124435.

Use of the Stanford Synchrotron Radiation Lightsource, SLAC National Accelerator Laboratory, is supported by the U.S. Department of Energy, Office of Science, Office of Basic Energy Sciences under Contract No. DE-AC02–76SF00515. The SSRL Structural Molecular Biology Program is supported by the DOE Office of Biological and Environmental Research, and by the National Institutes of Health, National Institute of General Medical Sciences (including P41GM103393). The contents of this publication are solely the responsibility of the authors and do not necessarily represent the official views of NIGMS or NIH. The Pilatus detector at beamline 4–2 at SSRL was funded under National Institutes of Health Grant S10OD021512.

Funding Sources

This work was supported by the National Institutes of Health (NIH) grant GM141799 (to C.K.) and National Cancer Institute, grant number P41 CA196276 and NSF-funded Science and Technology Center supported by NSF grant DBI1548297 to C.S.C.

REFERENCES

(1). Walsh C Polyketide and nonribosomal peptide antibiotics: modularity and versatility. Science 2004, 303, 1805–1810. [PubMed: 15031493]

(2). Katz L The DEBS Paradigm for Type I Modular Polyketide Synthases and Beyond. Methods Enzymol 2009, 459, 113–142. [PubMed: 19362638]

(3). Donadio S; Staver M; Mcalpine J; Swanson S; Katz L Modular organization of genes required for complex polyketide biosynthesis. Science 1991, 252, 675–679. [PubMed: 2024119]

(4). Khosla C; Herschlag D; Cane D; Walsh C Assembly Line Polyketide Synthases: Mechanistic Insights and Unsolved Problems. Biochemistry 2014, 53, 2875–2883. [PubMed: 24779441]

(5). Lowry B; Li X; Robbins T; Cane D; Khosla C A Turnstile Mechanism for Controlled Growth of Biosynthetic Intermediates on Assembly-Line Polyketide Synthases. ACS Central Science 2016, 2, 1, 14–20. [PubMed: 27163017]

(6). Cogan D; Li X; Sevillano N; Mathews I; Matsui T; Craik C; Khosla C Antibody Probes of Module 1 of the 6-Deoxyerythronolide B Synthase Reveal an Extended Conformation During Ketoreduction. J Am Chem Soc 2020, 142, 35, 14933–14939. [PubMed: 32786753]

(7). Akey D; Razelun J; Tehranisa J; Sherman D; Gerwick W; Smith J Crystal structures of dehydratase domains from the curacin polyketide biosynthetic pathway. Structure 2010, 18, 1, 94–105. [PubMed: 20152156]

(8). Keatinge-Clay A A tylosin ketoreductase reveals how chirality is determined in polyketides. Chem Biol 2007, 14, 8, 898–908. [PubMed: 17719489]

(9). Zheng J; Taylor C; Piasecki S; Keatinge-Clay A Structural and functional analysis of A-type ketoreductases from the amphotericin modular polyketide synthase. Structure 2010, 18, 8, 913–922. [PubMed: 20696392]

(10). Broadhurst R; Nietlispach D; Wheatcroft M; Leadlay P; Weissman K The structure of docking domains in modular polyketide synthases. Chem Biol 2003, 10, 723–731. [PubMed: 12954331]

(11). Klaus M; Rossini E; Linden A; Paithankar KS; Zeug M; Ignatova Z; Urlaub H; Khosla C; Köfinger J; Hummer G; Grininger M Solution structure and conformational flexibility of a polyketide synthase module. J Am Chem Soc 2021, 1, 12, 2162–2171.

(12). Li X; Sevillano N; La Greca F; Hsu J; Mathews I; Matsui T; Craik C; Khosla C Discovery and characterization of a thioesterase-specific monoclonal antibody that recognizes the 6-deoxyerythronolide B synthase. Biochemistry 2018, 57, 43, 6201–6208. [PubMed: 30289692]

(13). Bagde S; Mathews I; Fromme C; Kim C Asymmetric architecture of type I modular polyketide synthase revealed by X-ray and cryo-EM. Science 2021, 374, 6568, 723–729. [PubMed: 34735234]

(14). Cogan D; Zhang K; Li X; Li S; Pintilie GD; Roh SH; Craik C; Chiu W; Khosla C Mapping the catalytic conformations of an assembly-line polyketide synthase module. Science 2021, 374, 729–34. [PubMed: 34735239]

(15). Li X; Sevillano N; La Greca F; Deis L; Liu YC; Deller M; Mathews I; Matsui T; Cane D; Craik C; Khosla C Structure-Function Analysis of the Extended Conformation of a Polyketide Synthase Module. J Am Chem Soc 2018, 140, 6518–6521. [PubMed: 29762030]

(16). Smith JL; Skiniotis G; Sherman DH Architecture of the polyketide synthase module: surprises from electron cryo-microscopy. Current Opinion in Structural Biology, 2015, 31, 9–19. [PubMed: 25791608]

(17). Guzman K; Khosla C Fragment antigen binding domains (Fabs) as tools to study assembly-line polyketide synthases. Synth Syst Biotechnol 2022, 7, 506–512. [PubMed: 34977395]

(18). Wong FT; Chen AY; Cane DE; Khosla C Protein-Protein Recognition between Acyltransferases and Acyl Carrier Proteins in Multimodular Polyketide Synthases. Biochemistry, 2010, 49, 1, 95. [PubMed: 19921859]

(19). Chen AY; Schnarr NA; Kim CY; Cane DE; Khosla C Extender unit and acyl carrier protein specificity of ketosynthase domains of the 6-deoxyerythronolide B synthase. J Am Chem Soc. 2006, 128, 9, 3067–74. [PubMed: 16506788]

(20). Khosla T; Tang Y; Chen A; Schnarr N; Cane D Structure and Mechanism of the 6-Deoxyerythronolide B Synthase. Annual Review of Biochemistry 2007, 76, 195–221.

(21). Chen A; Cane D; Khosla C Structure-Based Dissociation of a Type I Polyketide Synthase Module. Chemistry & Biology 2007, 14, 7, 784–792. [PubMed: 17656315]

(22). Hans M; Hornung A; Dziarnowski A; Cane DE; Khosla C Mechanistic Analysis of Acyl Transferase Domain Exchange in Polyketide Synthase Modules. J Am Chem Soc. 2003, 125, 5366–5374. [PubMed: 12720450]

(23). Tang Y; Chen A; Kim CY; Cane D; Khosla C Structural and mechanistic analysis of protein interactions in module 3 of the 6-deoxyerythronolide B synthase. Chem Biol 2007, 14, 8, 931–943. [PubMed: 17719492]

(24). Dickinson M; Miyazawa T; McCool R; Keatinge-Clay A Priming enzymes from the pikromycin synthase reveal how assembly-line ketosynthases catalyze carbon-carbon chemistry. Structure 2022, 30, 9, 1331–1339. [PubMed: 35738283]

(25). Alekeyev V; Liu C; Cane D; Puglisi J; Khosla C Solution structure and proposed domain domain recognition interface of an acyl carrier protein domain from a modular polyketide synthase. Protein Sci 2007, 16, 2093–2107. [PubMed: 17893358]

(26). Kapur S; Chen AY; Cane DE; Khosla C Molecular recognition between ketosynthase and acyl carrier protein domains of the 6-deoxyerythronolide B synthase. Proc Natl Acad Sci USA 2010, 107, 22066–22071. [PubMed: 21127271]

(27). Wu J; Kinoshita K; Khosla C; Cane D Biochemical Analysis of the Substrate Specificity of the β-Ketoacyl-Acyl Carrier Protein Synthase Domain of Module 2 of the Erythromycin Polyketide Synthase. Biochemistry 2004, 43, 51, 16301–16310. [PubMed: 15610024]

(28). Gokhale R; Tsuji SY.; Cane, D.; Khosla, C. Dissecting and Exploiting Intermodular Communication in Polyketide Synthases. Science 1999, 284, 5413, 482–485. [PubMed: 10205055]

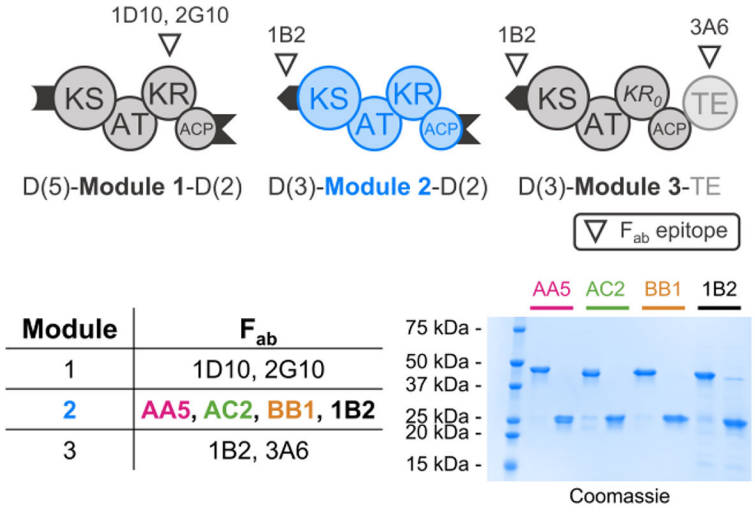

Figure 1.

F_{ab}s specific to distinct regions of DEBS Modules 1, 2 and 3 have been identified to date via phage display (top). SDS-PAGE analysis (bottom right) of purified F_{ab}s (AA5, AC2, and BB1) described in this report are shown under non-reducing (left lane) and reducing (right lane) conditions. For reference, a previously characterized F_{ab} (1B2) that binds specifically to the helical docking domain of Module 3 is also included.

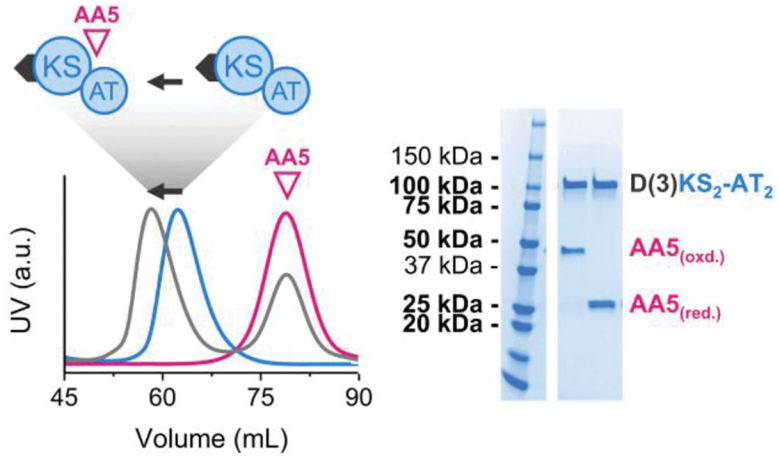

Figure 2.

1.5 molar equivalents F_{ab} AA5 were incubated with D(3)KS_2-AT_2 on ice for 1 h before injection onto a SEC column. Comparison of SEC UV Chromatographs of AA5 (pink), D(3)KS_2-AT_2 (blue), and AA5:D(3)KS_2-AT_2 (grey). SDS-PAGE analysis of the major SEC peak (grey) shows a near 1:1 stoichiometric mixture of AA5 and D(3)KS_2-AT_2.

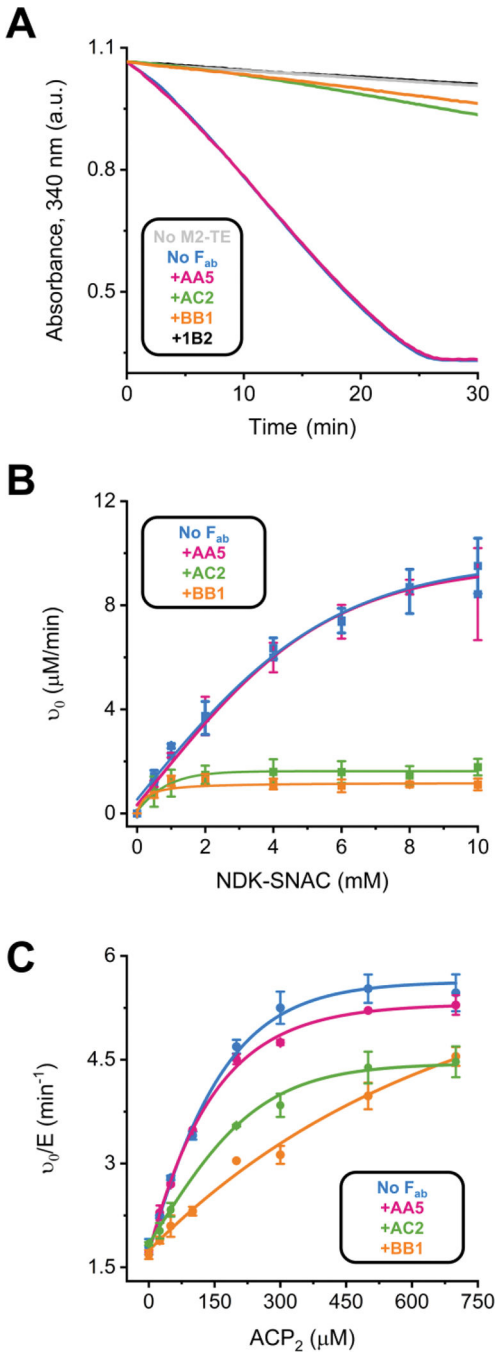

Figure 3.

(A) NADPH consumption by a truncated bimodular derivative of DEBS comprised of only its first two modules was monitored in the presence of 1.5 equivalents AA5 (pink), AC2 (green), BB1 (orange), or 1B2 (black). Control assays lacking M2-TE (grey) or any F_{ab} (blue) are also shown. (B) Effect of AA5, AC2, BB1, and 1B2 binding on DEBS Module 2-TE turnover at varied NDK-SNAC concentrations. (C) Effect of AA5 (5 μM), AC2 (5 μM) or BB1 (1 μM) on the activity of a dissociated form of Module 2 comprised of D(3)KS_2-

AT_2, KR_2, and varying concentrations of ACP_2. Data points correspond to averages of technical triplicates.

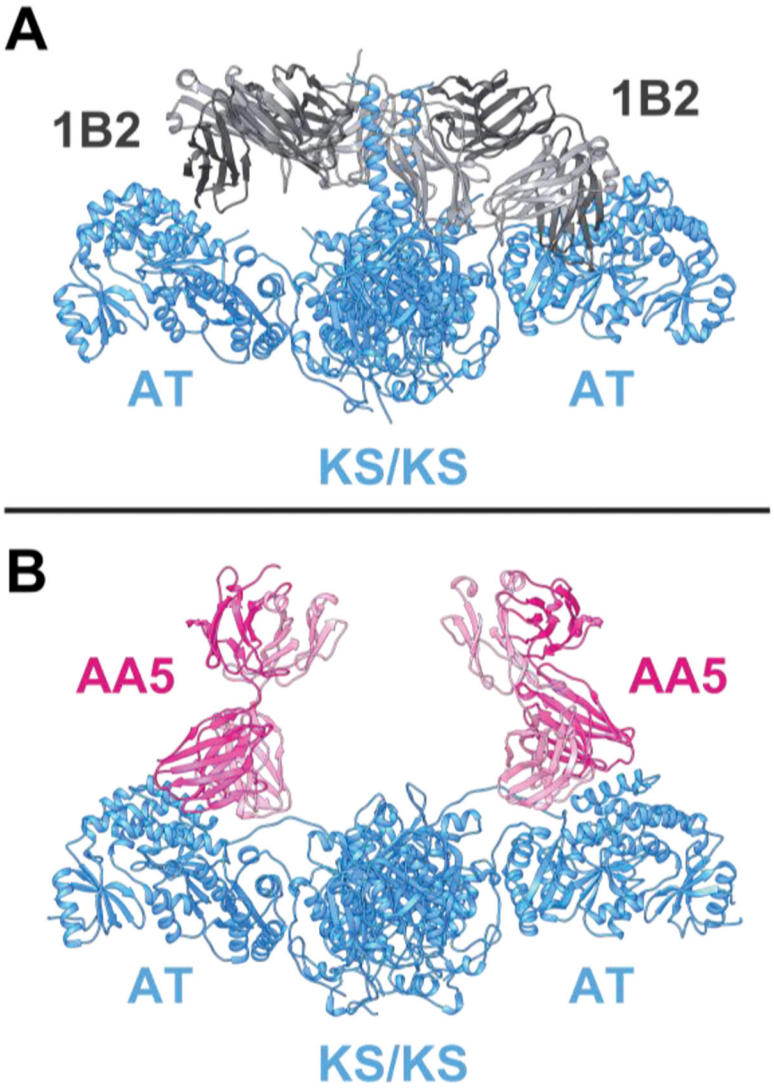

Figure 4.
Crystal structure(s) of (A) 1B2- (PDB ID 8EE0) and (B) AA5- (PDB ID 8EE1) bound D(3)KS_2-AT_2.